Frequency content of vertical ground vibrations caused by surface impact

Wersäll, C.
Department of Civil and Architectural Engineering, Royal Institute of Technology, Stockholm, Sweden

Bodare, A. & Massarsch, K. R.
Geo Risk & Vibration Scandinavia AB, Solna, Sweden

Wersäll, C. Bodare, A. and Massarsch, K. R., 2012. Frequency content of vertical ground vibrations caused by surface impact. The Ninth International Conference on Testing and Design Methods for Deep Foundations, IS-Kanazawa 2012, Japan, pp. 877 - 884.

Keywords: vibration, frequency, pile driving, impact, falling weight, shear wave, shear strain

ABSTRACT: Impact pile driving is often restricted by regulations of ground vibrations that affect surrounding structures, installations and residents. While previous studies have focused on prediction of vibration amplitude, this paper studies the frequency content. Vibrations can be particularly significant when the pile penetrates stiff surface layers. This phase is essentially analogous to impact of a falling weight on a steel plate, placed on the ground surface. Results from falling weight tests are evaluated with regard to frequency content of ground vibrations. Comparison of test results with theoretical models shows that the most important factors influencing dominating frequency of vertical ground vibration are pile dimensions, pile mass, and hammer mass. An often-neglected aspect is the dynamic stiffness of the soil immediately below the plate/pile toe while the influence of deeper soil layers on frequency content appears to be negligible. Soil modulus and wave speed are strain-dependent and the strain softening effect must be taken into consideration in the analysis. Results of field tests are compared with theory. The analogy between falling weight tests and pile driving, and its limitations are discussed.

1 INTRODUCTION

Although impact pile driving is a cost-effective foundation method, its efficient application in urbanized areas is often restricted by environmental regulations and, in particular, by limitations based on permissible ground vibrations. In spite of its wide application, relatively little effort has been devoted to development of practically applicable concepts to predict ground vibrations. Massarsch and Fellenius (2008) proposed a concept, which makes it possible to assess vibrations that are generated along the shaft and at the pile toe during pile penetration. However, this concept does not consider how the pile driving affects frequency content. One important aspect, which can be addressed in terms of frequency, is vibration amplification occurring in soil layers or buildings adjacent to the pile installation location. When the vibration frequency is in a certain range (commonly 10 to 20 Hz), it can coincide with resonance frequencies of building floors or structural elements. It is not uncommon that vertical and/or horizontal vibrations are amplified in buildings by many times (Athanasopoulos and Pelekis, 2000; Xia et al., 2005). This aspect is taken into account in several vibration standards, requiring that the project engineer assesses the risk of vibration amplification.

The dominating frequency caused by impact pile driving depends on the characteristics of the impacting system (pile, hammer etc.) as well as on soil properties. Figure 1 illustrates that the transfer of vibrations from the hammer (A), through the pile (B) and into the surrounding soil (C) is a complex process. Experience suggests that ground vibrations can be high in particular during the initial driving phase, when the pile penetrates a stiff soil layer or fill close to the ground surface. During this phase, the distance between the vibration source and adjoining buildings is shortest. The frequency content of ground vibrations caused by surface impact is analyzed theoretically and the significance of different driving parameters is discussed. Results from falling weight tests are compared to simulation of a simplified driving system, consisting of a mass impacting on a stiff plate/pile located at the ground surface. The results of field tests are compared with theoretical predictions. The consequences of strain softening on soil stiffness are addressed.

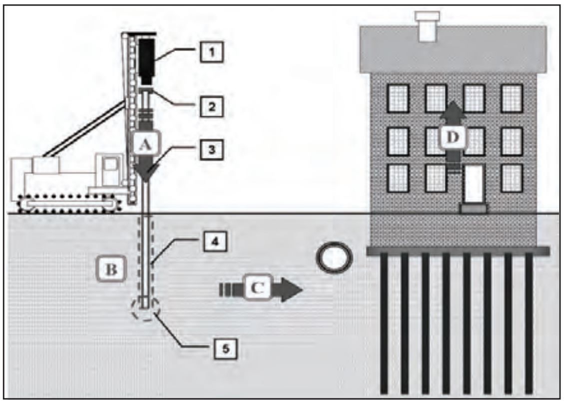

Figure 1. Process of energy transfer during pile driving, after Massarsch (2005).

2 DYNAMIC SOIL RESISTANCE

During pile penetration the shear modulus at large strain governs the dynamic soil resistance. This modulus is significantly lower than the small strain modulus measured by seismic tests. Figure 2 shows the shear modulus at different stress levels. The shear modulus at very low strain - typically less than 10^{-5} (0.001 %) - is denoted G_0 but decreases with increasing stress level. At 50 % of the failure load, the shear modulus is denoted G_{50} and at failure G_f. During pile penetration, soil at the pile-soil interface (toe) is in failure and the shear modulus G_f should be used, rather than the elastic shear modulus, G_0. This important aspect if often neglected and can lead to erroneous conclusions regarding dynamic soil resistance.

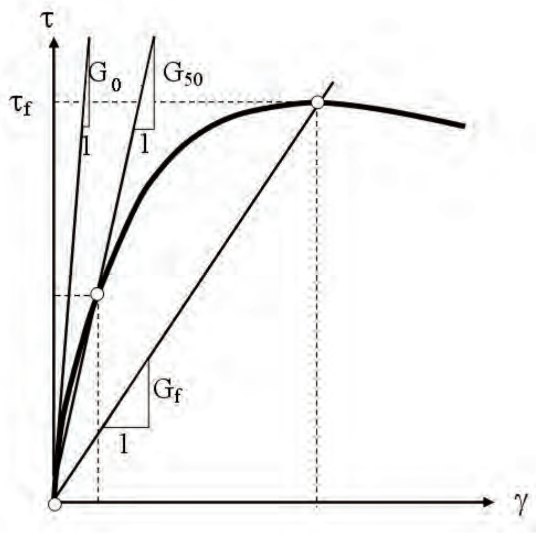

Figure 2. Shear stress-shear strain relationship for soil, after Massarsch (2004).

The shear modulus, G, can be calculated if the shear wave speed, c_S, and the bulk density of the soil ρ_{soil} are known,

$$G = c_S^2 \rho_{soil} \tag{1}$$

Ground vibrations due to impact pile driving are caused by the velocity-dependent soil resistance acting along the pile shaft and at the pile toe, (Massarsch and Fellenius 2008). The dynamic portion of the total driving resistance at the pile toe, R_T, which is of primary interest for a pile impacting at the ground surface, can be calculated from

$$R_T = 2 Z_P v^P \tag{2}$$

where Z_P is soil impedance for P-waves below the pile toe and v^P is particle velocity in the pile. Knowledge of the P-wave soil impedance, Z_P, is important for determination of the dynamic resistance at the pile toe-soil interface. The soil impedance, Z_P, is defined by

$$Z_P = A^P c_P \rho_{soil} \tag{3}$$

where A^P is cross section area of the pile toe and c_P is P-wave speed in the soil. In practice it is often more convenient to determine c_S and to calculate c_P from the following relationship

$$c_P = c_S \sqrt{\frac{2-2\upsilon}{1-2\upsilon}} \tag{4}$$

where ν is Poisson's ratio, which varies typically between 0.3 (drained conditions) and 0.5 (undrained conditions). Note that c_P depends on the degree of saturation of the ground water. In loose to medium dense, water-saturated soils, at undrained conditions, the compression wave speed corresponds to that in water (approximately 1450 m/s) and is of course independent of strain level.

In the case of pile penetration, the soil at the pile toe undergoes plastic deformation. The strain-dependent wave speed c^* can be determined from the elastic shear wave speed, c_S, by applying a wave speed reduction factor, R_c,

$$c^* = R_c c_S \tag{5}$$

Figure 3 shows the variation of the wave speed reduction factor R_c as a function of plasticity index, *PI*. The reduction becomes more significant as *PI* decreases. At failure, assuming a shear strain level of 1 %, c_S is reduced to approximately 15 % of the elastic speed in silty and sandy soils. When the soil fails, no additional resistance can be mobilized and this implies an upper limit of vibration intensity that can be transferred at the pile-soil interface. This effect is denoted “vibration transmission efficacy”, (Massarsch and Fellenius, 2008).

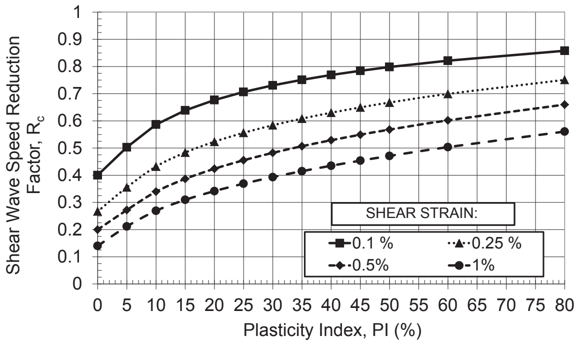

Figure 3. Reduction of c_S as a function of *PI* for cohesive soils for different shear strain levels, based on Massarsch (2004).

The soil immediately below the vibration source is in a plastic state. The frequency content of vibrations at the source depends on the dynamic response (i.e. shear wave speed) of the soil in this zone. In the present paper, this aspect is considered by calibrating calculations to field measurements, which confirm a reduced shear wave speed. With increasing distance, shear strain decreases and thus shear wave speed increases. However, this change in wave speed does not affect the frequency content of propagating vibrations as it is the frequencies generated at the source that propagate through the soil.

3 FALLING WEIGHT TESTS

As a part of a project to investigate ground conditions by seismic methods of an area with heterogeneous ground conditions, falling weight tests (SASW method, among others) were performed using a purpose-built 1000 kg steel mass, dropped on a steel impact plate (Figure 4). Rubber pads of varying thickness were placed between the plate and the weight to study a possible damping effect. These measurements were used to investigate the effect of ground conditions on impact-induced ground vibration frequency.

3.1 Ground conditions

Ground conditions within the test area were variable and the influence of dynamic soil properties on dynamic response and frequency content could therefore be studied in detail. Conditions varied from 3 m of stiff glacial till on bedrock in one part of the test area to soft, very compressible clay, up to 20 m thick, elsewhere. A surface layer of 2-3 m of rockfill was placed over the entire area.

Figure 4. Falling weight tests.

3.2 Test setup

Several drops were made at 33 locations using varying drop height and thickness of rubber padding. Some drops were also made without the impact plate. The standard setup was 0.5 m drop height and 50 mm rubber pads. Signals were averaged in frequency domain over several drops to eliminate noise. Both accelerometers and geophones were used for measurement, placed in sand-filled pits to assure good coupling with the ground. Measurements presented in this paper consist of vertical velocity or acceleration recorded at a horizontal distance of approximately 5 m from the impact point.

3.3 Results

All average velocity spectra from tests using geophones according to the standard test setup are shown in Figure 5. The amplitudes are influenced by test conditions with a few curves having considerably larger amplitudes. This variation is probably also influenced by slight variation in the distance between impact point and transducer location. The variation of vibration amplitude is not of primary interest for this paper. Although vibration amplitudes vary at different tests, it is interesting to note that dominating frequencies fall within a relatively narrow range (generally 25-30 Hz), regardless of geotechnical conditions and variation of soil stiffness below the surface layer of rockfill. Thus, vibration frequency appears to be less influenced by test conditions than vibration amplitude.

Several tests were also performed to investigate the variation of specific test parameters. Figure 6 shows average spectra for two different drop heights, 0.5 and 0.9 m, and Figure 7 shows the influence of rubber pad thickness (keeping all other parameters constant). There is a remarkable similarity between the different spectra, suggesting that the varied parameters do not affect the frequency content of vertical ground vibrations. In Figure 8, standard drops of 0.5 m are compared with 1 m drops without using the impact plate. Also here, the difference in measured frequency content is negligible.

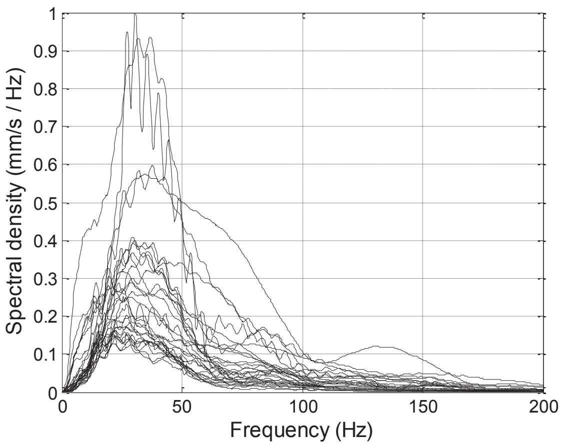

Figure 5. Average velocity spectra at all drop points.

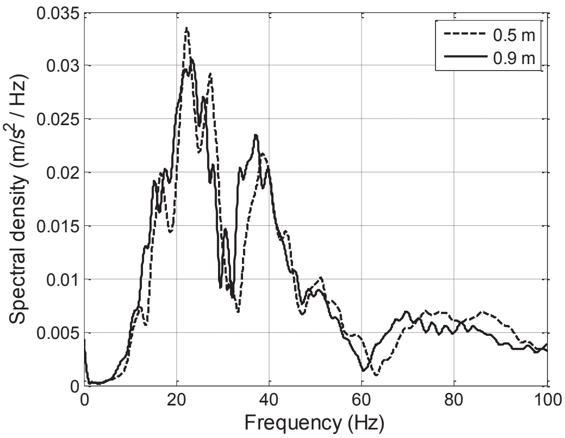

Figure 6. Influence of drop height.

4 LUMPED-PARAMETER MODEL

Surface impact has been modeled using a lumped-parameter SDOF model. Three different versions of the model have been analyzed: *(a)* falling weight system, *(c)* pile-hammer system and *(b)* intermediate model, see Figure 9. The dynamic response of the ground can be derived by considering impact and soil interaction separately.

The three models are similar, with varying geometries of system components. Models *(a)* and *(b)* consider the impact of a falling weight and of a pile on a plate supported by ground with stiffness and damping. Model *(c)* simulates a hammer impacting on a pile supported by the ground.

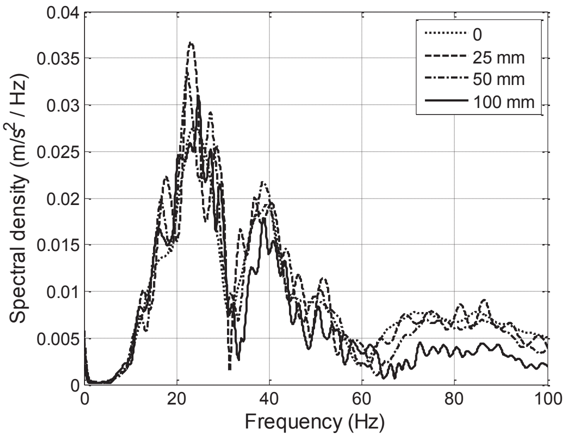

Figure 7. Influence of rubber pad thickness.

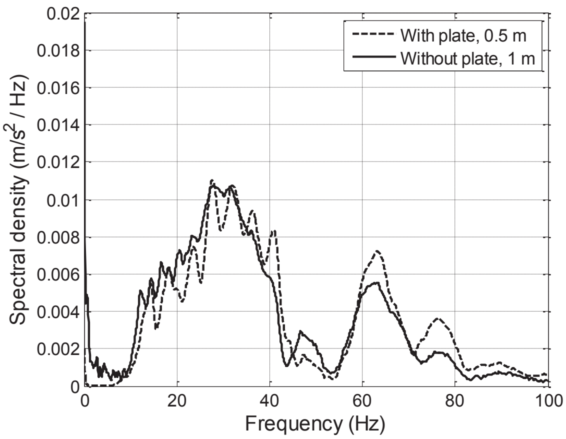

Figure 8. Acceleration spectra with and without plate.

4.1 Impact

When the falling weight impacts the plate, an upward propagating wave is induced in the steel weight and a downward wave in the plate/pile. The time for the wave to travel up and down in the weight, plate, or pile is a characteristic time of the system and its corresponding frequency. For the models analyzed herein, this frequency range is 600-4200 Hz, which is well above that of interest for ground vibrations. The weight, pile, and impact plate can therefore be modeled as rigid bodies.

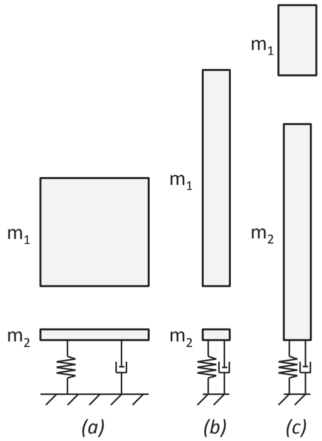

Figure 9. The three different SDOF models.

The displacement, u, of the SDOF system is described by the differential equation, Eq. 6.

$$m\frac{d^2u}{dt^2}+c\frac{du}{dt}+ku=mg \tag{6}$$

where m is the total mass (m_1+m_2), c is the damping coefficient, k is the spring stiffness and g is the gravity acceleration. The initial conditions are that, at time t = 0, displacement is zero and velocity is some value, v_0. The velocity of the falling weight at impact is

$$v_1=\sqrt{2gH} \tag{7}$$

where H is drop height. Using the principle of conservation of momentum and assuming elastic rebound, the velocity of the plate/pile after impact is

$$v_0=v_1\frac{2m_1}{m_1+m_2} \tag{8}$$

where m_1 and m_2 are the masses of the falling weight and the plate/pile, respectively.

Assuming fully elastic rebound implies a coefficient of restitution of unity. In reality, the coefficient is slightly lower. Although a more representative value would be important for determining the vibration amplitude, it is less significant for assessing the frequency content. Since frequency is of main interest in this paper, elastic rebound is considered an acceptable assumption.

A short duration after rebound, the weight will reverse direction and again hit the plate, this time with significantly less energy. This is of minor importance for the dominating frequencies as discussed below. The solution to Equation (6) for the initial conditions is

$$u(t)=e^{-\zeta\omega_0 t}\left[-\frac{mg}{k}\cdot\cos\left(\omega_d\cdot t\right)+\frac{\omega_0\cdot v_0-\zeta g}{\omega_0^2\cdot\sqrt{1-\zeta^2}}\cdot\sin\left(\omega_d\cdot t\right)\right]+\frac{mg}{k} \tag{9}$$

where ζ is damping ratio, which is the ratio of damping coefficient and critical damping coefficient. The natural frequency, ω_0, and the damped natural frequency, ω_d, are obtained from

$$\omega_0=\sqrt{\frac{k}{m}} \tag{10}$$

$$\omega_d=\omega_0\sqrt{1-\zeta^2} \tag{11}$$

4.2 Soil interaction

Soil-plate interaction is considered by using interaction parameters that take both the rigid mass and the deformable soil into account. According to Lysmer and Richart (1966) and Richart et al. (1970), the elastic spring stiffness and damping ratio can be expressed by

$$k=\frac{4\cdot G\cdot r_0}{1-\nu} \tag{12}$$

$$\zeta=0.425\cdot\sqrt{\frac{4\rho\cdot r_0^3}{\left(1-\nu\right)\cdot m}} \tag{13}$$

where G is soil shear modulus, r_0 is plate radius, ν is Poisson's ratio for the soil, and ρ is soil density.

4.3 Frequency analysis

The solution to Equation (6) is of the form

$$f\left(t\right)=e^{-\zeta\omega_0\cdot t}\left[A\cos(\omega_d\cdot t)+B\sin(\omega_d\cdot t)\right] \tag{14}$$

which has the Fourier transform

$$F\left(\omega\right)=A\cdot\frac{\zeta\omega_0-i\omega}{\left(\zeta\omega_0-i\omega\right)^2+\omega_d^2}+B\cdot\frac{\omega_d}{\left(\zeta\omega_0-i\omega\right)^2+\omega_d^2} \tag{15}$$

Differentiating Equation (9) with respect to time and applying Equation (15) results in the velocity spectral density

$$V(\omega)=\left|\frac{v_0\cdot(2\zeta\cdot\omega_0+i\omega)-g}{\omega_0^2-\omega^2+2i\zeta\omega_0\omega}\right| \tag{16}$$

Equation (16) is used to calculate velocity spectra in the following sections.

4.4 *Adjustment for strain level*

As has been discussed above, the wave speed needs to be adjusted to take into account the influence of strain level. This aspect is of particular importance when the applied dynamic force causes the falling weight or pile to penetrate into the underlying soil. Reducing the shear modulus (i.e. c_S) decreases the dominating frequency and increases amplitude, cf. Equations (10) and (12). By varying c_S in the model until the dominating frequency coincides with that observed in the falling weight tests, an estimation of the strain-adjusted (reduced) wave speed is obtained. Hence, this method makes it possible to calibrate the theoretical model against field tests and measured frequencies.

5 COMPARISON OF FIELD TESTS WITH THEORETICAL MODEL

SASW tests performed in the test area showed that the shear wave speed in the 3 m thick surface rockfill is about 200-250 m/s over the entire test area. Figure 10 shows variation of frequency content for different values of c_S for model *(a)* (falling weight). At c_S=100 m/s, a dominating frequency of 28 Hz is obtained, agreeing well with field measurements (cf. Figure 5). This frequency corresponds to a wave speed reduction factor of R_C=0.4–0.5. Hence, c_S=100 m/s should be used as strain-adjusted shear wave speed in rock fill. As illustrated in Figure 10, the frequency content strongly depends on c_S, and, therefore, also the magnitude of strain. This aspect is discussed further below.

5.1 *Comparison of models*

Using the adjusted shear wave speed for all three models, frequency content according to Figure 11 is obtained. Spectral density is plotted in logarithmic scale due to the large difference in amplitude. The curve for model *(a)* is calculated by inserting the same mass (1000 kg) and diameter (600 mm) as in the field experiments and a 20 mm thick plate with the same diameter. In model *(b)*, the diameter is changed to 200 mm (cf. Figure 9) but the mass of the falling weight is the same as in model *(a)* (1000 kg), corresponding to a pile length of approximately 4 m. The masses are then interchanged in model *(c)* so that the falling weight has the same mass as the plate in the previous model, 5 kg, and a 1000 kg pile (impact plate).

Comparing models *(a)* and *(b)* in Figure 11, it can be seen that decreasing the diameter while keeping the mass constant significantly increases amplitude and decreases dominating frequency. This is due to a drastic decrease in damping, cf. Equation (13). The dominating frequencies in models *(b)* and *(c)* are identical since the total system mass and the diameter (hence damping) are the same. There is, however, a large difference in amplitude, which is due to the difference in momentum (mass times velocity) of the falling mass.

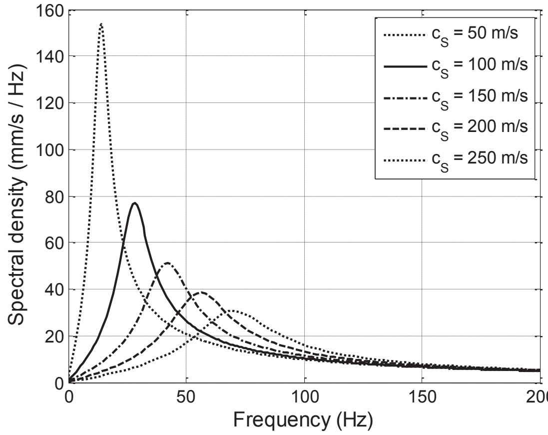

Figure 10. Calculated velocity spectrum with varying shear wave speed.

5.2 *Hammer mass*

In the previous example, a 5 kg hammer was used, which is an unrealistically low mass for a pile hammer. **Figure 12** shows influence of hammer mass, with a 1000 kg pile having a diameter of 200 mm. It can be seen that both amplitude and dominating frequency are affected. Higher hammer mass gives rise to higher amplitude. Dominating frequencies converge and range for this case between 7 and 17 Hz. The mass of a typical pile hammer ranges between 2500 and 4000 kg. In this interval, the dominating frequency is relatively constant (7-9 Hz).

5.3 *Bouncing*

Directly after impact, the plate will move downward with a higher velocity than the hammer. After a short time, there will be a second impact and the weight will keep bouncing on the plate. The kinetic energy is reduced significantly after each impact and is considered negligible after the second impact. Hence, only the first two impacts are considered. If the weight is heavier than the plate, it will also move downward after impact. However, if it is lighter, it will have a velocity directed upward. Bouncing is here calculated by a simplified approach, assuming that the second impact of a light hammer occurs at the same location (same height) as the first impact. Bouncing in case of a heavy hammer is not considered, because the energy of the second impact will be very low compared to the initial impact.

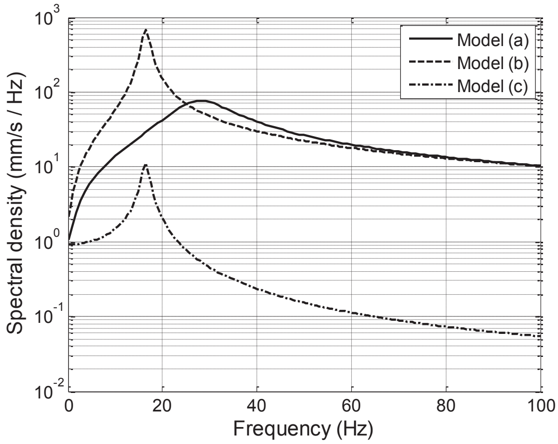

Figure 11. Comparison of the three models.

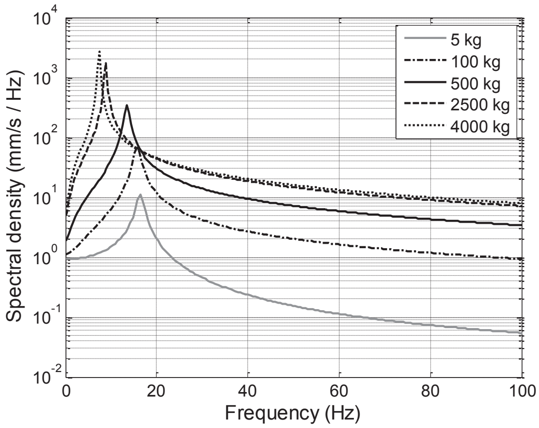

Figure 12. Influence of hammer mass on frequency.

The influence of bouncing is shown in Figure 13 for a 100 kg hammer and in Figure 14 for a 500 kg hammer. The pile has a mass of 1000 kg. Bouncing has greater influence when the hammer is light compared to the pile, owing to the greater rebound height.

6 DISCUSSION AND CONCLUSIONS

Field tests show that a falling weight with a mass of 1000 kg impacting a steel plate (1 m in diameter) on ground consisting of 2-3 m of rockfill induces ground vibrations with frequency content that is almost independent of the soil conditions below a depth exceeding 2-3 m. It can be concluded that the dominating frequency is not strongly influenced by stiffness of material at larger depth. This agrees well with the widely appreciated conception that the dynamics of a vibrating footing depend on soil conditions to a depth of 2.5-3 times the footing diameter (e.g., Baidya and Krishna 2001).

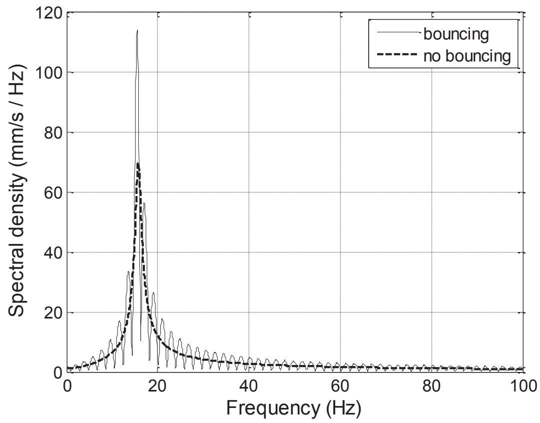

Figure 13. Influence of bouncing for a 100 kg hammer.

Theoretical analyses also suggest that components of the driving system such as hammer drop height and hammer mass are of minor importance for the frequency content of vertical ground vibrations.

An interesting observation of the field tests is that ground vibration amplitude remains almost unchanged even when drop height is increased by nearly 100 percent. This can be explained by the fact that during plastic penetration, an upper limit of dynamic soil resistance (shear modulus at failure) is reached. Thus, during pile penetration, vibration amplitude depends on the dynamic soil resistance at the plate/soil interface (pile toe) and becomes at failure almost independent of the applied force. This fact has been observed previously (e.g., Andréasson and Hansbo 1977, and Massarsch and Fellenius 2008).

However, when the applied force is smaller than the soil ultimate resistance below the pile toe, penetration will decrease and can result in higher dynamic stiffness and thus increased ground vibrations (e.g., during the final seating of the pile on a bearing stratum).

The above results suggest that frequencies generated by impact depend primarily on the dynamic characteristics of the weight/hammer-pile system and on the ground conditions immediately below the plate/pile toe. Whether the three meter thick, stiff rock fill is underlain by very soft clay or by dense glacial till appears to have minor influence on frequency content.

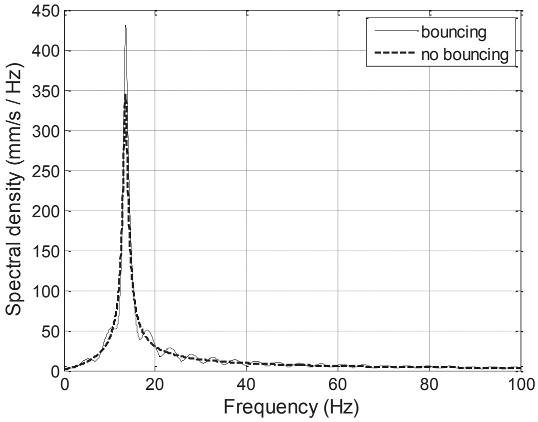

Figure 14. Influence of bouncing for a 500 kg hammer.

The main difference between frequencies generated by a weight falling on a steel plate and impact pile driving is the diameter of the plate (pile). The influence of these geometrical differences has been investigated in the lumped-parameter model.

The calibrated model shows good agreement with measured frequency spectra from field tests. The frequencies considered herein are sufficiently low to justify the assumption that almost no change in frequency content takes place between the point of impact and the measuring point. However, there is naturally a significant decrease in amplitude (thus explaining the large difference in the amplitude observed in field tests as opposed to results from simulations).

Decreasing the diameter of the plate to 200 mm and increasing the mass to 1000 kg produces a system which is similar to impact pile driving. Reducing the diameter changes the damping in the system and decreases the dominating frequency. Furthermore, increasing hammer mass also decreases the dominating frequency. For a given pile and typical masses of pile driving hammers (2500-4000 kg), the dominating frequency range is relatively narrow.

Bouncing of the hammer produces a spectrum that follows the trend of the original spectrum, but has a more irregular shape. The maximum amplitude can be affected by bouncing, but not the general shape of the spectrum. Bouncing effects are therefore considered to have minor influence on the frequency content.

In order to account for the strain softening effect due to plate penetration, the shear wave speed of 200-250 m/s in the surface layer (rock fill) must be reduced to 100 m/s, corresponding to a mean wave speed reduction factor of $R_C = 0.44$, implying a shear strain on the order of 10^{-3} to 10^{-2} (0.1 – 1.0 %).

7 ACKNOWLEDGEMENTS

The work presented in this paper would not have been possible without the valuable discussions with Dr. Bengt H. Fellenius who also reviewed the manuscript and offered valuable contributions. The valuable comments by one of the reviewers is acknowledged.

REFERENCES

Athanasopoulos, G.A. and Pelekis, P.C. (2000): "Ground vibrations from sheetpile driving in urban environment: measurements, analysis and effects on buildings and occupants", Soil Dynamics and Earthquake Engineering, 19(5), pp.371-387.

Andréasson, B. and Hansbo, S. (1977): "Compaction control by dynamic methods", Väg- och vattenbyggaren, Stockholm, No 8-9, 3 p.

Baidya, D.K. and Krishna, G.M. (2001): "Investigation of Resonant Frequency and Amplitude of Vibrating Footing Resting on a Layered Soil System", Geotechnical Testing Journal, 24(4), pp.409-417.

Lysmer, J. and Richart, F.E., Jr. (1966): "Dynamic response of footings to vertical loading", J. of the Soil Mech. and Found. Div., ASCE, 92(1), pp.65-91.

Massarsch, K.R. (2004): "Deformation properties of fine-grained soils from seismic tests. Keynote lecture", International Conference on Site Characterization, ISC'2, Porto, 19 – 22 Sept. 2004, Porto, pp.133-146.

Massarsch, K.R. (2005): "Ground Vibrations Caused by Impact Pile Driving. Invited Lecture", Proceedings, Environmental Vibrations: Prediction, Monitoring, Mitigation and Evaluation (ISEV 2005). Okayama University, Japan, September 20–22, 2005, Taylor & Francis, pp. 369 - 379.

Massarsch, K.R. and Fellenius, B.H. (2008): "Ground vibrations induced by impact pile driving", The Sixth International Conference on Case Histories in Geotechnical Engineering, Edited by S. Prakash, Missouri University of Science and Technology, August 12 16, 2008, Arlington, Virginia, 38 p.

Richart, F.E., Jr., Hall, J.R., Jr. and Woods, R.D. (1970): Vibrations of soils and foundations, Prentice-Hall, Englewood Cliffs, New Jersey. 414 p.

Xia, H., Zhang, N. and Cao, Y.M. (2005): "Experimental study of train-induced vibrations of environments and buildings", Journal of Sound and Vibration, 280, pp.1017-1029.